Title

Hepatocyte Nicotinamide Adenine Dinucleotide Phosphate Reduced Oxidase 4 Regulates Stress Signaling, Fibrosis, and Insulin Sensitivity During Development of Steatohepatitis in Mice

Journal

Gastroenterology, 149(2)

ISSN

0016-5085

Authors

Bettaieb, Ahmed

Jiang, Joy X

Sasaki, Yu

et al.

Publication Date

2015-08-01

DOI

10.1053/j.gastro.2015.04.009

Peer reviewed

HHS Public Access

Author manuscript

Gastroenterology. Author manuscript; available in PMC 2016 August 01.

Published in final edited form as:

Gastroenterology. 2015 August ; 149(2): 468–480.e10. doi:10.1053/j.gastro.2015.04.009.

Hepatocyte NADPH Oxidase 4 Regulates Stress Signaling, Fibrosis, and Insulin Sensitivity During Development of Steatohepatitis in Mice

Ahmed Bettaieb[1], **Joy X. Jiang**[2], **Yu Sasaki**[2], **Tzu-I Chao**[2], **Zsofia Kiss**[2], **Xiangling Chen**[2], **Jijing Tian**[2], **Masato Katsuyama**[3], **Chihiro Yabe-Nishimura**[3], **Yannan Xi**[1], **Cedric Szyndralewiez**[4], **Kathrin Schröder**[5], **Ajay Shah**[6], **Ralph P. Brandes**[5], **Fawaz G. Haj**[1], and **Natalie J. Török**[2]

[1]Department of Nutrition, UC Davis, Davis, CA, USA [2]Department of Medicine, Gastroenterology and Hepatology, UC Davis, Sacramento, CA [3]Kyoto Prefectural University of Medicine, Kyoto, Japan [4]Genkyotex, Geneva, Switzerland [5]Wolfgang Goethe University, Frankfurt am Main, Germany [6]King's College London British Heart Foundation Centre, London, UK

Abstract

Background & Aims—Reactive oxidative species (ROS) are believed to be involved in the progression of non-alcoholic steatohepatitis (NASH). However, little is known about the sources of ROS in hepatocytes or their role in disease progression. We studied the effects of NADPH oxidase 4 (NOX4) in liver tissues from patients with NASH and mice with steatohepatitis.

Methods—Liver biopsy samples were obtained from 5 patients with NASH, as well as 4 patients with simple steatosis and 5 patients without steatosis (controls) from the University of California,

Correspondence: Natalie Török, M.D., UC Davis Medical Center, Patient Support Services Building, 4150 V Street, Suite 3500, Sacramento, CA 95817. njtorok@ucdavis.edu; fax: 916-734-7908.

Authorship Note: Ahmed Bettaieb and Joy X. Jiang contributed equally to this work.

Author's involvement in the manuscript: Ahmed Bettaieb: performing experiments
Joy X. Jiang: performing experiments and writing paper
Yu Sasaki: performing experiments
Tzu-I Chao: performing experiments
Zsofia Kiss: performing experiments
Xiangling Chen: performing experiments
Jijing Tian: performing experiments
Masato Katsuyama: collaboration, technical support
Chihiro Yabe-Nishimura: collaboration
Yannan Xi:performing experiments
Cedric Szyndralewiez: collaboration
Kathrin Schröder: collaboration, technical support
Ralph P. Brandes: collaboration, technical support
Ajay Shah: technical support
Fawaz G. Haj: collaboration, technical support
Natalie J Török: concept and design, analysis of the data, funding

Disclosures: Nothing to disclose

Author names in bold designate shared co-first authorship

Davis Cancer Center Biorepository. Mice with hepatocyte-specific deletion of NOX4 (*NOX4*^{hepKO}) and *NOX4*$^{floxp+/+}$ C57BL/6 mice (controls) were given fast food diets (supplemented with high-fructose corn syrup) or choline-deficient L-amino acid-defined to induce steatohepatitis, or control diets, for 20 weeks. A separate group of mice were given the NOX4 inhibitor (GKT137831). Liver tissues were collected and immunoblot analyses were performed determine levels of NOX4, markers of inflammation and fibrosis, double-stranded RNA-activated protein kinase (PKR), and phospho-eIF-2alpha kinase (PERK)-mediated stress signaling pathways. We performed hyperinsulinemic-euglycemic clamp studies and immunoprecipitation analyses to determine the oxidation and phosphatase activity of PP1C.

Results—Levels of NOX4 were increased in patients with NASH, compared with controls. Hepatocyte-specific deletion of NOX4 reduced oxidative stress, lipid peroxidation, and liver fibrosis in mice with diet-induced steatohepatitis. A small molecule inhibitor of NOX4 reduced liver inflammation and fibrosis and increased insulin sensitivity in mice with diet-induced steatohepatitis. In primary hepatocytes, NOX4 reduced the activity of the phosphatase PP1C, prolonging activation of PKR and PERK-mediated stress signaling. Mice with hepatocyte-specific deletion of NOX4 and mice given GKT137831had increased insulin sensitivity.

Conclusion—NOX4 regulates oxidative stress in the liver and its levels are increased in patients with NASH and mice with diet-induced steatohepatitis. Inhibitors of NOX4 reduce liver inflammation and fibrosis and increase insulin sensitivity, and might be developed for treatment of NASH.

Keywords

mouse model; stress signaling; obesity; inflammation

With the obesity epidemic non-alcoholic fatty liver disease (NAFLD)/non-alcoholic steatohepatitis (NASH) are becoming the most common liver diseases[1, 2]. The progression of NAFLD to NASH is characterized by a necroinflammatory process with hepatocyte ballooning, lipoapoptosis and progressive fibrosis. Patients with type II diabetes and obesity are at high risk of developing inflammation and fibrosis but the mechanistic events connecting insulin resistance to the progression of liver disease and fibrosis are not well understood. Oxidative stress is a key feature of NASH however, the main cellular and enzymatic sources of the oxidative radicals or the mechanism of their action have not been fully investigated [3]. Recently, NADPH oxidases (NOXs) received a considerable attention as major producers of reactive oxidative species (ROS). NOXs play a significant pathogenic role in cardiovascular disease, diabetes and diabetes-induced nephropathy [4-8] thus their role in NASH has to be investigated. Of the seven NOX homologue enzymes, NOX4 could have a key importance as it was recently shown to be instrumental in diabetic nephropathy [8]. In the liver NOX4 is expressed in hepatocytes [9], activated stellate cells (HSC) [10, 11], to a small extent in sinusoidal endothelial cells while Kupffer cells do not express it [12]. We and others have recently shown that NOX4 activation in HSC is profibrogenic [10, 11]. In hepatocytes however, the role of NOX4 has not been defined in *in vivo* studies; and if targeting NOX4 becomes an antifibrogenic approach its role in the parenchymal cells needs to be addressed. The induction of ER stress pathways in hepatocytes is an important determinant of cell fate as activation of the unfolded protein response (UPR) in the case of a mild or temporary

stress can result in the restoration of homeostasis whereas prolonged insults can lead to the activation of the mitochondrial pathway of apoptosis[13-15]. As to how protracted oxidative stress in hepatocytes is linked to the activation of stress signaling has not been well characterized. The double-stranded RNA-activated protein kinase (PKR) is a stress kinase, classically known to be activated by dsRNA, viral proteins, and polyanionic compounds [16]. Redox signals were described to modulate both PKR [17] and PERK [18] potentially affecting their target eIF2α leading to propagation of ER stress. On the other hand PKR can regulate insulin signaling in physiological states and in obesity[19, 20]. Therefore NOX4/PKR/PERK in hepatocytes could be key proximal elements at the crossroads of controlling inflammatory and stress responses linked to metabolic activity.

Here we report that NOX4 is induced in patients with NASH and in two dietary animal models causing necroinflammation and pericellular fibrosis analogous to human NASH. By using a novel loss-of function mouse model for hepatocyte NOX4 we uncovered that NOX4 is implicated in the induction and persistence of PKR/PERK activation in NASH livers by the inactivation of the PP1c phosphatase, leading to the propagation of ER stress with CHOP and JNK1/2 activation and hepatocyte cell death, driving fibrosis. NOX4 inhibition by the GKT137831 compound (Genkyotex) resulted in a significant reduction in inflammation and fibrosis. Our results also demonstrate a NOX4-mediated negative effect on hepatocyte insulin signaling with the attenuation of IR, IRS-1 and Akt phosphorylation and decreasing insulin sensitivity. Overall, our studies highlight the proximal role of NOX4 in liver injury, fibrosis and hepatic insulin resistance in NASH, and have important implications regarding new treatment strategies preventing progressive liver disease.

Materials and Methods

Reagents

Antibodies for p-PKR (Thr451, Millipore), PKR, eIF2α, p-eIF2α (Ser51), p-PERK (Thr980), PERK, CHOP, caspase 3, PKR and IR were from Santa Cruz Biotechnology (Santa Cruz, CA). The well-characterized primary antibody for NOX4 was a kind gift from Dr. A. Shah (King's College London British Heart Foundation Centre, London)[21], p-JNK (Thr183/Tyr185), JNK, p-AKT (Ser473) and AKT were obtained from Cell Signaling Technology (Danvers, MA). Antibodies for p-IRE1α (Ser724) and PTP1B were purchased from Abcam (Cambridge, MA). Antibodies for p-IRS1 (Tyr608) and IRS1 were from Millipore Corp. (Billerica, MA). Antibodies for pIR (Tyr1162/Tyr1163) were from Invitrogen (Carlsbad, CA). PVDF membranes and protein standards were obtained from BIO-RAD (Hercules, CA). The enhanced chemiluminescent (ECL) detection reagents were from Thermo Fisher Scientific Inc. (Piscataway, NJ). The antibodies used are listed in Table 1.

Human biopsy samples

The liver biopsy samples were obtained from the UC Davis Cancer Center Biorepository funded by the NCI. This study was exempt from IRB review as de-identified samples were used. Samples from 5 different NASH patients, 4 patients with simple steatosis and 5 normal livers were tested. The patients with fibrotic NASH or simple steatosis were from the

bariatric patient population with a mean BMI (46.2+/-5.8), and mean HOMA (7.1 ± 10.6)[22]. The precise BMI and HOMA for each patient are not known as these were de-identified samples.

Results

NOX4 is induced in patients with NASH and in mice fed fast food or CDAA diets

NOX4 is a transcriptionally regulated enzyme not requiring the assembly of cellular subunits and is mainly producing H_2O_2 [23]. To address if NOX4 induction during NASH could be a significant source of ROS; RTqPCR experiments and immunohistochemistry were performed on the liver biopsy samples from NASH patients, patients with simple steatosis, and healthy livers, and in two animal models of NASH. The patients with NASH or simple steatosis were morbidly obese. The BMI of the patients with normal livers was in the normal range. NOX4 mRNA was significantly increased in NASH patients, compared to those with simple steatosis, or healthy controls (Figure 1A, N=5). Hepatocytes in the liver biopsy samples from NASH patients exhibited a strong NOX4 signal (Figure 1B, insert). On confocal images of these livers there was colocalization of NOX4 to e-cadherin positive hepatocytes, αSMA positive activated HSC, but not to CK19 positive cholangiocytes (Suppl. Fig. 1, we have used a polyclonal antibody obtained from Dr. Shah[21]. To study NOX4 expression we used two different murine models of NASH. The fast food diet (FFD) was shown to recapitulate the calorie intake and composition of that of the human diet linked to NASH[24]. The CDAA diet model is known to result in weight gain, insulin resistance and histological changes consistent with NASH in contrast to MCD diet[25]. The advantage of using the CSAA/CDAA model is that the CSAA arm of this diet only induces steatosis without inflammation or fibrosis resembling NAFLD with simple steatosis. In both the FFD and CDAA models the mice gain significant amount of weight, and develop insulin resistance; histologically steatosis, necroinflammation and pericellular fibrosis are observed[25, 26]. NOX4 was induced at mRNA and protein levels in the FFD fed mice (Figure 1C, D), and on the CDAA dietary model after 20 weeks whereas no induction was seen on the CSAA diet (Figure 1E).

Oxidative stress, lipid peroxidation and fibrosis are decreased in the NOX4^{hepKO} mice

To investigate the role of NOX4 in oxidative injury during NASH, we generated conditional knockout mice by crossing NOX4*fl/fl* with Alb-cre mice to delete NOX4 from hepatocytes. These mice were viable and showed no obvious anomalies. NOX4^{hepKO} mice and littermate *fl/fl* controls were fed chow, FFD or CSAA/CDAA diets. There was an increase in body weight that was similar in both genotypes (Suppl. Fig. 2A), and the liver/body weight ratios showed no significant difference between the genotypes. Serum ALT was significantly reduced in the NOX4^{hepKO} mice on both diets (Figure 2A, and Suppl. Fig. 3A) whereas bilirubin was not affected (data not shown). Oxidative radicals were reduced by 83% in the NOX4^{hepKO} mice and lipid peroxidation was also attenuated in both dietary models in the conditional knockouts (Figure 2B, C and Suppl. Fig. 3B, C). In addition we observed significant improvement in necroinflammation and the downregulation of TNF-α, MCP1 and Il-β in the NOX4^{hepKO} mice in the FFD diet, and TNF-α, MCP1 in the CDAA diet (Figure 2E and Suppl. Fig. 3E). As lipoapoptosis of hepatocytes is a major driving force for

fibrosis in NASH[27,28]; we assessed the expression of the active caspase 3 subunit by immunofluorescence (5 different fields/sample) and by western blot (Figure 5). There was decreased activation of caspase 3 and apoptosis in the NOX4^{hepKO} livers on both diets (Fig. 2F, Suppl. Fig. 3D and Fig. 5).

Liver fibrosis, an important feature of NASH progression; was significantly attenuated in both dietary models in the NOX4^{hepKO} mice; as assessed by hydroxyproline assay (Figure 3A, and Suppl. Fig. 4A), picrosirius red staining and Image J analysis (Figure 3B, and Suppl. Fig. 4B). The expression of procollagen α1(I), αSMA and TGF-β studied by RTqPCR (FFD: Figure 3C, D, E; CDAA diet: Suppl. Fig. 4C, D, E) were all downregulated in the NOX4^{hepKO} mice.

Liver steatosis (H&E and oil red staining), and triglyceride content showed no significant difference between the genotypes on the FFD (Suppl. Figure 5A, B, C). The serum triglyceride values were also not significantly different (data not shown). Expression of the lipogenic transcripts SREBP1c, FAS, PPARγ increased, as expected after the FFD (Suppl. Fig. 5D) however; there was no significant difference between the genotypes. Only the expression of the fatty acid translocase CD36 was downregulated in the NOX4^{hepKO} mice on both diets (Suppl. Figure 5D, and Suppl. Fig. 6F). The steatosis and triglyceride content improved in the NOX4^{hepKO} mice on the CDAA diet along with the attenuation of the lipogenic transcripts SREBP1c, FAS, PPARγ and CD36 expression (Suppl. Fig. 6).

Inhibition of NOX4 by GKT137831 improves inflammation and fibrosis in fast food diet-fed mice

To address if pharmacological inhibition of NOX4 could reverse histological changes and/or reduce inflammation or fibrosis in NASH, we used GKT137831, a small molecule NOX1/4 inhibitor that in previous models was shown to reduce fibrosis in the BDL[10] or CCl4[29] models. Mice on the FFD were gavaged from week 6 of the 12 week diet with the inhibitor or the vehicle. There was a significant improvement in ALT, (Figure 4A), inflammatory markers (Figure 4B), fibrosis and fibrogenic transcripts (Figure 4C, D). In addition, there was an improvement in overall insulin sensitivity in the inhibitor-treated group (Figure 4E). Body weight and liver/body weight ratios were not significantly different between the groups (Suppl. Data 2B).

NOX4 induces hepatocyte stress signaling pathways in vivo and in vitro

To elucidate the key pathways induced by NOX4-mediated oxidative stress in hepatocytes, we focused on the role of PKR/PERK, central stress kinases whose activity could be affected by changes in redox conditions[17, 18]. We observed increased phosphorylation (Thr451) of PKR and PERK (Thr980) in the *fl/fl* mice on FFD that was attenuated in NOX4^{hepKO} mice (Figure 5, densitometry). The activity of the downstream signaling target eIF2-α was also significantly decreased in the FFD fed NOX4^{hepKO} mice compared to controls. Sustained JNK activation is an important determinant of hepatocyte injury and cell death[30] and JNK1 has been described as a downstream target of PKR[31, 32] thus our next step was to evaluate its phosphorylation in both dietary models. We observed attenuated CHOP,

JNK1/2 and caspase 3 activation in the livers of FFD fed NOX4^{hepKO} mice compared to controls (Figure 5, and Suppl. Fig. 7, N=5).

In primary hepatocytes palmitate mediates NOX4 induction and the decrease in PP1c phosphatase activity

To investigate the mechanism of NOX4 activation in hepatocytes, primary cells were transfected with a construct containing the human NOX4 promoter, and treated with palmitate a saturated fatty acid known to cause ER stress[27]. To analyze the palmitate-mediated induction we focused on a TGFβ a known inducer of the NOX4[33]. We observed a significant induction in the NOX4 promoter activity (Figure 6A) that was reduced by DNSmad3. As positive control, TGFβ-mediated induction is shown. In contrast, oleic acid, an unsaturated fatty acid did not induce promoter activity (Fig. 6B). In NOX4$^{-/-}$ hepatocytes the palmitate-mediated CHOP activation decreased both at the mRNA (Fig. 6C) and protein level; and caspase 3 activation was also blunted (Figure 6D). The decreased activation of caspase 3 was consistent with the attenuated hepatocyte apoptotic cell death seen in both *in vivo* models. In oleic acid-treated cells there was no induction of CHOP or caspase 3 activation noted (Figure 6D). Next, we focused on the mechanism by which NOX4 activation and H_2O_2 release leads to an enhanced PKR phosphorylation. Type 1 protein phosphatases have previously been shown to dephosphorylate and inactivate PKR and PERK, and of these PP1c was described as the most efficient[34]. We tested the phosphatase activity of PP1c after immunoprecipitating from palmitate-exposed hepatocytes of NOX4*fl/fl* mice in the presence or absence of glutathione (GSH) or H_2O_2; or from the NOX4$^{-/-}$ mice. Activity of PP1c was significantly reduced in NOX4*fl/fl* cells treated with palmitate that was restored by GSH (Figure 6E). Treatment with H_2O_2 also induced a significant attenuation of phosphatase activity. In contrast, there was no reduction in the PP1c activity after palmitate in the NOX4$^{-/-}$ hepatocytes owing to the reduced oxidation and improved activity of the phosphatase.

Insulin sensitivity and signaling are improved in the NOX4^{hepKO} mice

The data showing decreased stress signaling in the NOX4^{hepKO} mice raised the possibility that insulin responses in the livers of these mice were affected, as well. To explore this, we performed glucose and insulin tolerance tests in mice after 12 weeks on the FFD, and found that the NOX4^{hepKO} mice had overall improved glucose tolerance and insulin sensitivity (Figure 7A, B).

To study insulin signaling; *fl/fl* or NOX4^{hepKO} mice on the FFD were given insulin, and immunoprecipitation/western blot performed to assess IR, IRS-1, and western blot Akt phosphorylation. On the FFD phosphorylation of IR$^{Tyr1162/Tyr1163}$, IRS-1^{Tyr608}, and Akt^{Ser473} were improved in the NOX4^{hepKO} mice compared to controls fed FFD (Figure 7C, densitometry). To evaluate the respective roles of NOX4 and JNK1 playing in modulating insulin signaling, we transduced primary, WT or JNK1 KO hepatocytes with Ad-GFP (control), or Ad-NOX4, and exposed them to insulin. Ad-NOX4 reduced insulin-mediated IRS-1^{Tyr608} and Akt^{Ser473} phosphorylation in JNK1KO hepatocytes compared to control-transduced cells, suggesting that NOX4/H_2O_2 exerts JNK1-independent effects in dysregulating insulin signaling (Fig. 7D).

To further analyze hepatic insulin resistance, hyperinsulinemic-euglycemic studies were performed on wt (*fl/fl*) and NOX4^{hepKO} mice on 12w of FFD after overnight fast. During the clamp, the glucose infusion rate (GIR) required to maintain euglycemia was greater for the NOX4^{hepKO} mice (Suppl. Figure 8A, B), suggesting improved whole-body insulin sensitivity. The analysis also demonstrated that insulin had no effect on hepatic glucose output (HGP) in the WT mice, indicating hepatic insulin resistance (Suppl. Figure 8C). In contrast, insulin reduced HGP compared to basal rates in the NOX4^{hepKO}, suggesting preserved insulin action compared to wt mice. Plasma glucose levels were matched. (Suppl. Fig. 8D). The glucose uptake was unchanged (Suppl. Fig. 8E). The clamped insulin values were matched between the groups (Suppl. Fig. 8F).

Discussion

Type II diabetes mellitus is a known clinical risk factor for developing progressive steatohepatitis yet the mechanisms linking altered insulin signaling to the fibrogenic activity in the liver have not been well elucidated. Dysregulation of key adaptive responses such as ER stress have been described in several studies in NASH [15, 35, 36]. While these studies have resulted in a better understanding of the molecular regulation of the UPR and the signaling cross talks between the different branches of ER stress pathways, many questions remain on the proximal initiating events. In this paper we explored the role of hepatocyte NOX4 as a key source of oxidative radicals regulating the progression of NASH. Our data in two animal models show that specific deletion of NOX4 in hepatocytes or its inhibition using the small molecule NOX4 inhibitor protects against fibrosis, and interestingly, against dysregulated hepatic insulin sensitivity characteristic of metabolic liver injury.

There have been several sources of oxidative radicals described in hepatocytes in NASH [3, 37, 38] but their overall contribution to disease progression *in vivo* has not been well defined. NOXs are an important group of enzymes responsible for producing either superoxide by respiratory burst in phagocytic cells or H_2O_2 by NOX4 [23]. We have previously described the role of the phagocytic NOX2 in stellate cell and Kupffer cells and its link to liver fibrogenesis[39]. NOX2 can also mediate an increased TNFα converting enzyme (TACE) activity in these cells thereby leading to the activation of TNFα [40]. NOX4 a non-phagocytic NOX has been described to play a role in the fibrogenic activation of HSC [10, 11]. In hepatocytes NOX4 is an important source of sustained H_2O_2 release [11] but its role in NASH has not been addressed. We found that the expression of NOX4 was significantly increased in livers of NASH patients and in two animal models with corresponding increase in ROS production. Importantly, the deletion of NOX4 from hepatocytes or its pharmacological inhibition by a small molecule inhibitor was protective against fibrosis. Hepatocyte apoptosis is a well-known inducer of fibrogenic activation of HSC either by the release of DAMPS or the phagocytosis of apoptotic debris that directly activates stellate cells [39, 41]. We have earlier shown that NOX4 plays a role in FasL or TNFα-mediated apoptosis of hepatocytes in the bile duct ligation (BDL) model [10]. In the study of Carmona-Cuenca et al. NOX4 mediated the proapoptotic effects of TGFβ *in vitro* [42]. As hepatocyte apoptosis is intimately linked to a progressive fibrogenic activity in the liver [43-45] we next addressed how NOX4 with H_2O_2 release affects downstream stress pathways resulting in apoptosis and how this impacts on fibrosis progression. We have

focused on the PKR and PERK branch of stress signaling as these kinases are important targets of ROS modulation. FFD or CDAA diet led to increased phosphorylation of PKR and PERK in control mice that was significantly attenuated in NOX4^{hepKO} mice. As PKR/PERK deemed to be important instigator kinases [46-48] and were recently described to play a role in inflammasome activation [49]; an important question is how their activity is sustained by NOX4. While several members of the PP1 group of phosphatases may play a role in controlling PKR/PERK activity, PP1c was attributed the strongest phosphatase activity[34]. PP1c is also known to be an eIF2α phosphatase therefore its oxidation could amplify downstream ER signaling. PP1c activity was significantly reduced by palmitate or H_2O_2 however; no reduction was seen in the NOX4$^{-/-}$ hepatocytes, signifying that the oxidation was NOX4 dependent.

Deleting NOX4 from hepatocytes has led to improved insulin responses *in vivo*. We have detected an improvement in insulin effects in the NOX4^{hepKO} mice already after 12 weeks on the diet at a time that precedes the development of significant inflammation, apoptosis and fibrosis in this model [24] pointing to the early role of NOX4 in NASH pathogenesis. Prior data in terms of ROS-mediated effects on insulin signaling in hepatocytes were contradicting. This, in part stems from the fact that NOX/ROS-mediated effects were mainly studied in cell culture models including cancer cell lines where the physiological insulin responses and anti-oxidant pathways are altered. *In vivo* in normal state constitutive low level of NOX4 activation and the released H_2O_2 as a second messenger could be an important positive regulator of insulin signaling by inhibiting the protein-tyrosine phosphatase 1B (PTP1B), that targets IR signaling [50, 51]. In pathological events such as NASH however, the persistently and significantly increased levels of ROS could lead to oxidative conformational changes of several crucial phosphatases such as TCPTP, another important regulator of insulin action[52]; or PPIs that allow PKR, PERK and eIF2α to be increasingly activated. Active PKR is known to bind to IRS-1 inducing its serine phosphorylation and decreasing insulin signaling[19]. The regulatory role of PKR activity in insulin responsiveness was also supported by a recent publication by Nakamura et al. where using small molecule inhibitors of PKR improved glucose homeostasis in mice [20]. In addition, the attenuated JNK1/2 signaling observed in our study could also be providing a positive feedback for insulin sensitivity in the NOX4^{HepKO} mice. We observed however, that JNK1 was only partially involved in the NOX4-mediated dampening of insulin effects thus other key pathways including, but not limited to PKR/PERK could also be instrumental in the redox regulation of insulin sensitivity. The dynamics and hierarchy of pathways by which sustained NOX4 activation can reduce insulin sensitivity in the liver should be addressed in future studies. NOX4 deletion from hepatocytes did not affect weight gain. While obesity and adipose inflammation are causative factors in inflammatory signaling in the liver; the degree of obesity is not necessarily in linear correlation with histological progression [53]. Thus dysregulation of redox conditions in the liver can modulate inflammatory and fibrogenic activity in NASH.

An important question is whether other NOXs could achieve the same effect on hepatic stress signaling and insulin sensitivity. Deletion of the phagocytic NOX2 reduced oxidative stress and ameliorated vascular dysfunction in insulin resistant mice[54]. Although NOX2 a

phagocytic NOX is expressed in hepatocytes, it is unclear how it is induced or whether it affects hepatocyte ER stress. Similarly, the role of NOX1 a non-phagocytic homologue, in NASH remains to be studied, and this is especially important as NOX1/4 inhibition in our study showed protection. Although our data suggest an improvement of insulin resistance in the inhibitor-treated mice; further studies are warranted to test the effects of the NOX4 inhibitor on all tissues that play a role in glucose homeostasis. Compensatory activation of other NOXs in our system would also be plausible however, the significant decrease in oxidative radicals in the $NOX4^{hepKO}$ mice points to the key role of NOX4. An interesting finding was that the deletion of NOX4 in hepatocytes resulted in a distinct effect on steatosis and lipogenesis in the two dietary models. In the choline-deficient model where lipogenesis plays a major role, NOX4 could exert a differential transcriptional effect on lipogenic genes (e.g. PPARγ that is known to be redox-regulated). In addition, CIDEC/Fsp27 could also be affected by redox regulation leading to modulation of triglyceride content[55]. The downregulation of fatty acid transporter CD36 was consistent in our study and future work would be required to address the mechanism of its $NOX4/H_2O_2$-mediated regulation.

Our work describes the central role of increased redox signaling that instigates insulin resistance in the liver in early NASH, whereas later this propagates to hepatocytes stress injury and fibrogenesis. These events are governed by an increased NOX4 expression and activity, leading to the activation of PKR/PERK key stress kinases that are at the crossroad of stress signaling and modulation of insulin sensitivity. The spatial-temporal relationship between these pathways is just emerging and further work is needed to fully understand these cross talks. As NOX4 also mediates stellate cell activation, NOX4 inhibition could be a potential treatment approach in NASH mitigating hepatocyte cell death, fibrosis and improving insulin sensitivity.

Animal models, diets

$NOX4floxp^{+/+}$ mice with C57BL/6 background were generous gifts from Dr. Kathrin Schröder (Wolfgang Goethe University, Germany)[23]. The $NOX4floxp^{+/+}$ mice were bred with C57BL/6 Albumin-Cre mice (Jackson) to create NOX4 hepatocyte-specific knockout ($NOX4^{hepKO}$) mice. Progenies with NOX4 depleted in hepatocytes were selected by genotyping using Cre recombinase primers (F: GCGGTCTGGCAGTAAAAACTATC; R: GTGAAACAGCATTGCTGTCACTT). 6 week (w) old male $NOX4floxp^{+/+}$ *(fl/fl)* or $NOX4^{hepKO}$ mice were given control chow diet, choline sufficient L-amino acid defined (CSAA, 518753, Dyets Inc., Bethlehem PA), choline deficient L-amino acid defined (CDAA, 518754, Dyets Inc.) or fast food diet (FFD, #1810060, TestDiet, Richmond IN supplemented with high fructose corn syrup in the drinking water with a final concentration of 42 g/l.)[24] for 20 weeks. The ingredients of this diet are in Suppl. Table 2.

A group of C57BL/6 mice were fed the FFD, as above for 12 weeks, and were gavaged daily with GKT137831 (Genkyotex, Geneva, Switzerland) dissolved in 1.2w% Methylcellulose + 0.1w% Polysorbate 80 in water, (60 mg/kg), from week 6 of the feeding (therapeutic protocol). Control mice were gavaged with the vehicle. At the end of the experiments, serum samples from all animals were collected for ALT testing (BioVision Inc., Milpitas, CA). The liver samples were collected for histological analysis, quantitative real-time PCR (qRT-

PCR), and western blotting. The animals were housed in facilities approved by the National Institute of Health. All procedures were reviewed and approved by the Animal Welfare Committee of the University of California Davis.

Insulin tolerance test (ITT)

Insulin sensitivity of the *fI/fI* and NOX4^{hepKO} mice on chow diet or FFD was tested by using the ITT. After 12 weeks of FFD feeding mice were fasted and the weight of each animal was measured. Insulin (Novolin R) was administered (1 mU/g, i.p.) and blood glucose levels were measured at 0, 15, 30, 60, and 90 minutes.

Glucose tolerance test (GTT)

At the end of the 12th week on the FFD, the mice were fasted (with available water supply) for 16 hours the day before the experiment. D-glucose (Sigma-Aldrich) was given by intraperitoneal injection at 2 g/kg body weight. Blood glucose was measured 0, 15, 30, 60, and 120 minutes after the injection.

Hyperinsulinemic, euglycemic clamp studies

Mice were allowed to recover for one week prior to clamp experiments following surgical implantation of an indwelling catheter in the right jugular vein[25]. After an overnight fast, mice were infused with 3-[^{3}H]glucose at a rate of 0.05 μCi/min for 120 min to determine basal glucose turnover. A primed infusion of insulin and 3-[^{3}H]glucose was administered at 7.14 mU kg−1 · min−1 and 0.24 μCi/min, respectively, for 4 min, after which the rates were reduced to 3 milliunits·kg−1·min−1 insulin and 0.1 μCi/min 3-[^{3}H] glucose for the remainder of the experiment. Blood was collected via tail massage for plasma glucose, insulin, and tracer levels, and a variable infusion of glucose was given to maintain euglycemia. Following collection of the final blood sample, the mice were anesthetized with an intravenous injection of 150 mg/kg pentobarbital, and tissues were harvested and froze with aluminum forceps in liquid nitrogen. All of the tissues were stored at −80 °C until later use.

Histological analysis, immunohistochemistry

The human liver samples were fixed in 4% paraformaldehyde, embedded in paraffin, sectioned, and the slides were rehydrated prior to HE or Picrosirius red staining. Oil red staining was done on frozen samples. For immunodetection, the slides were exposed to citrate buffer (pH=6) for antigen retrieval. After blocking non-specific binding the slides were probed with primary anti-NOX4 antibody at 4°C overnight. The samples were reacted with biotinylated 2nd antibody before using 3,3′-Diaminobenzidine (DAB) (Abeam) as chromogen for signal detection. Imaging was performed by using a Zeiss Axioplan2 optical microscope (Carl Zeiss MicroImaging) with a charge-coupled device (CCD) camera. For immunofluorescent studies on mouse samples we used the NOX4 antibody obtained from Dr. A. Shah.

Isolation of primary hepatocytes and promoter assays

Primary hepatocytes were isolated and cultured in Williams E medium as described26. The cells were transfected with the pGL-hNOX4-Luc (gift from Dr. C. Yabe, Kyoto University) using the JetPEI reagent (Polyplus Transfection) then transduced with Ad- DNSmad 3 or Ad-GFP ($10E^5$/ml), 24 hours prior to treatment with 200 μm palmitate-BSA, BSA, or TGFβ1 (5ng/ml) for 16 hours and luciferase assays were performed.

Reverse transcription and quantitative real-time PCR (RTqPCR)

Total cellular RNA was collected using RNeasy mini kit (Qiagen, Valencia CA) according to the user's guide. cDNA was synthesized by using the iScript™ cDNA synthesis kit (Bio-Rad). RTqPCR experiments were performed using SYBR green PCR master mix (Applied Biosystems) in a 7900 HT RTPCR system (Applied Biosystems, Grand Island, NY). The RTqPCR primers are listed in Table 3 (Supplement). B2M (β2 microglobulin, human for formalin fixed paraffin embedded tissues) or Arbp (acidic ribosomal phosphoprotein, murine samples) were used as housekeeping gene.

Hydroxyproline assay

Hydroxyproline assays were performed as described[10]. In brief, the mouse liver tissue was homogenized and denatured. The hydrolyzed samples were dried and resuspended then incubated in chloramine T oxidation buffer (50 mM) for 20 minutes at room temperature. 3.15M of perchloric acid (Sigma-Aldrich) was added to react at room temperature for 5 min before the addition of p-dimethylaminobenzaldehyde (Sigma-Aldrich). The absorbance of each sample was measured at 557 nm.

Lucigenin assay

Membrane concentrates were obtained by ultracentrifugation at 10,000g then incubated with lucigenin (5μM, Life Technologies, Grand Island, NY) at room temperature for 15 min. 100μm NADPH (Sigma-Aldrich) added and the lucigenin intensity read by a luminometer.

Malondiadehyde (MDA) assay

Quantification of lipid peroxidation was conducted by using the thiobarbituric acid-reactive substances kit (Abeam) according to the manufacturer's manual. Liver samples were homogenized on ice in MDA lysis buffer before centrifugation then the supernatant was collected and incubated with thiobarbituric acid (TBA) solution at 95°C for 1hr. The absorbance was measured at 532 nm.

Triglyceride measurement

Liver triglycerides were measured by using the triglyceride colorimetric assay kit (Cayman Chemical, Ann Arbor MI). In brief, the liver tissue was homogenized in diluent buffer containing protease inhibitors before centrifugation at 1000 g for 10 minutes at 4°C. The supernatant was collected and diluted. The samples and the standards were added to a 96 well plate to react with the enzyme solution for 15 minutes and the absorbance was measured at 530-550 nm.

Western blot analyses

The mouse liver tissues were homogenized in RIPA buffer supplemented with protease inhibitors and phosphatase inhibitors (10 mM Tris-HCl, pH 7.4, 150 mM NaCl, 0.1% sodium dodecyl sulfate, 1% TritonX-100, 1% sodium deoxycholate, 5 mM EDTA, 1 mM NaF, 1 mM sodium orthovanadate and protease inhibitors). The lysates were collected and after protein assays SDS-PAGE was performed and the proteins were transferred to PVDF membranes. Membranes were blocked with 5% bovine serum albumin (BSA) and reacted with the relevant primary antibodies. Proteins were detected and visualized by using Luminata Forte western HRP substrate (EMD Millipore). For the insulin signaling experiments, animals were fasted overnight, injected i.p. with insulin (10 mU/g body weight), and sacrificed 10 minutes after injection. The livers were immediately frozen in liquid nitrogen. Protein concentrations were determined and proteins (500-1000 μg) were immunoprecipitated with anti-IRβ and anti-IRSl antibodies. Immune complexes were collected on protein G-Sepharose beads (GE Healthcare) and washed three times with lysis buffer. Proteins were resolved by SDS-polyacrylamide gel electrophoresis and transferred to nitrocellulose membranes. Immunoblots were performed with the antibodies mentioned earlier. For quantitation purposes, pixel intensities of immuno-reactive bands from blots that were in the linear range of loading and exposure were quantified using FluorChem 9900 (Alpha Innotech, CA).

PP1c activation assays

Primary hepatocytes were treated with palmitate-BSA (200 μM), BSA alone, H_2O_2 (10μm) or palmitate plus glutathione (5mM) and the cell lysates were collected by using NP40 cell lysis buffer (150Mm NaCl, l%NP-40, 10Mm Tris-HCl, 5% glycerol, 1mM EDTA, pH 7.4) supplemented with protease inhibitor cocktail (Roche). 2 μg of anti-PPlc-γ Ab (abl6387, Abeam) and protein G beads (sc-2002, Santa Cruz Biotechnology, Inc.) were added to 500 μg of total cell lysates for immunoprecipitation overnight at 4°C. After centrifugation the precipitates were resuspended in 50 μl of 1× colorimetric phosphatase activity assay buffer, and exposed to the substrate, p-nitrophenyl phosphate (pNPP) (N1891, Sigma-Aldrich) (5 mM), for 45 minutes. 20 μl of NaOH (5N) was added to stop the reaction and the activity of PPlC-γ was analyzed by recording the absorbance at 405 nm. For the PTP1B activity assay we used 1 mg of total lysates to immunoprecipitate with PureProteome beads (Millipore). The precipitate was washed twice with ice-cold lysis buffer and then resuspended in 50 μl of reaction buffer (50 mM HEPES (pH 5.0), 1 mM EDTA, 100 mM NaCl and 5 mM DTT) for 10 min, and then p-nitrophenyl phosphate (5 mM) was added. PTP1B activity was monitored by measuring the absorbance of p-nitrophenyl phosphate at 405 nm using a plate reader.

Statistical Analysis

All of the data represented at least three independent experiments and are presented as mean + standard error of the mean (SEM). The differences between multiple groups were compared using the analysis of variance (ANOVA) with Dunnett's test. The two-tailed, unpaired Student's t-test was used to analyze the differences between two groups. $P<0.05$ was considered statistically significant.

Supplementary Material

Refer to Web version on PubMed Central for supplementary material.

Acknowledgments

Yale MMPC funded by DK059635

Grant Support: This study was supported by the DK083283 and 01BX002418 (NJT), and DK095359 (FGH). YS was partially funded by the Jinsei Medical Foundation.

References

1. Bohinc BN, Diehl AM. Mechanisms of disease progression in NASH: new paradigms. Clin Liver Dis. 2012; 16:549–65. [PubMed: 22824480]
2. Masuoka HC, Chalasani N. Nonalcoholic fatty liver disease: an emerging threat to obese and diabetic individuals. Ann N Y Acad Sci. 2013; 1281:106–22. [PubMed: 23363012]
3. Feldstein AE, Bailey SM. Emerging role of redox dysregulation in alcoholic and nonalcoholic fatty liver disease. Antioxid Redox Signal. 2011; 15:421–4. [PubMed: 21254858]
4. Bedard K, Krause KH. The NOX family of ROS-generating NADPH oxidases: physiology and pathophysiology. Physiol Rev. 2007; 87:245–313. [PubMed: 17237347]
5. Altenhofer S, Kleikers PW, Radermacher KA, et al. The NOX toolbox: validating the role of NADPH oxidases in physiology and disease. Cell Mol Life Sci. 2012; 69:2327–43. [PubMed: 22648375]
6. Zhang M, Perino A, Ghigo A, et al. NADPH oxidases in heart failure: poachers or gamekeepers? Antioxid Redox Signal. 2013; 18:1024–41. [PubMed: 22747566]
7. Gorin Y, Block K. Nox as a target for diabetic complications. Clin Sci (Lond). 2013; 125:361–82. [PubMed: 23767990]
8. Gorin Y, Block K. Nox4 and diabetic nephropathy: With a friend like this, who needs enemies? Free Radic Biol Med. 2013; 61C:130–142. [PubMed: 23528476]
9. de Mochel NS, Seronello S, Wang SH, et al. Hepatocyte NAD(P)H oxidases as an endogenous source of reactive oxygen species during hepatitis C virus infection. Hepatology. 2010; 52:47–59. [PubMed: 20578128]
10. Jiang JX, Chen X, Serizawa N, et al. Liver fibrosis and hepatocyte apoptosis are attenuated by GKT137831, a novel NOX4/NOX1 inhibitor in vivo. Free Radic Biol Med. 2012; 53:289–96. [PubMed: 22618020]
11. Sancho P, Mainez J, Crosas-Molist E, et al. NADPH oxidase NOX4 mediates stellate cell activation and hepatocyte cell death during liver fibrosis development. PLoS One. 2012; 7:e45285. [PubMed: 23049784]
12. Paik YH, Iwaisako K, Seki E, et al. The nicotinamide adenine dinucleotide phosphate oxidase (NOX) homologues NOX1 and NOX2/gp91(phox) mediate hepatic fibrosis in mice. Hepatology. 2011; 53:1730–41. [PubMed: 21384410]
13. Nishitoh H. CHOP is a multifunctional transcription factor in the ER stress response. J Biochem. 2012; 151:217–9. [PubMed: 22210905]
14. Brenner C, Galluzzi L, Kepp O, et al. Decoding cell death signals in liver inflammation. J Hepatol. 2013; 59:583–94. [PubMed: 23567086]
15. Malhi H, Kaufman RJ. Endoplasmic reticulum stress in liver disease. J Hepatol. 2011; 54:795–809. [PubMed: 21145844]
16. Williams BR. PKR; a sentinel kinase for cellular stress. Oncogene. 1999; 18:6112–20. [PubMed: 10557102]
17. Li G, Scull C, Ozcan L, et al. NADPH oxidase links endoplasmic reticulum stress, oxidative stress, and PKR activation to induce apoptosis. J Cell Biol. 2010; 191:1113–25. [PubMed: 21135141]
18. Higa A, Chevet E. Redox signaling loops in the unfolded protein response. Cell Signal. 2012; 24:1548–55. [PubMed: 22481091]

19. Carvalho-Filho MA, Carvalho BM, Oliveira AG, et al. Double-stranded RNA-activated protein kinase is a key modulator of insulin sensitivity in physiological conditions and in obesity in mice. Endocrinology. 2012; 153:5261–74. [PubMed: 22948222]
20. Nakamura T, Arduini A, Baccaro B, et al. Small-molecule inhibitors of PKR improve glucose homeostasis in obese diabetic mice. Diabetes. 2014; 63:526–34. [PubMed: 24150608]
21. Anilkumar N, Weber R, Zhang M, et al. Nox4 and nox2 NADPH oxidases mediate distinct cellular redox signaling responses to agonist stimulation. Arterioscler Thromb Vasc Biol. 2008; 28:1347–54. [PubMed: 18467643]
22. Medici V, Ali MR, Seo S, et al. Increased soluble leptin receptor levels in morbidly obese patients with insulin resistance and nonalcoholic fatty liver disease. Obesity (Silver Spring). 2010; 18:2268–73. [PubMed: 20448542]
23. Lambeth JD. NOX enzymes and the biology of reactive oxygen. Nat Rev Immunol. 2004; 4:181–9. [PubMed: 15039755]
24. Charlton M, Krishnan A, Viker K, et al. Fast food diet mouse: novel small animal model of NASH with ballooning, progressive fibrosis, and high physiological fidelity to the human condition. Am J Physiol Gastrointest Liver Physiol. 2011; 301:G825–34. [PubMed: 21836057]
25. Miura K, Kodama Y, Inokuchi S, et al. Toll-like receptor 9 promotes steatohepatitis by induction of interleukin-1beta in mice. Gastroenterology. 2010; 139:323–34 e7. [PubMed: 20347818]
26. Kodama Y, Kisseleva T, Iwaisako K, et al. c-Jun N-terminal kinase-1 from hematopoietic cells mediates progression from hepatic steatosis to steatohepatitis and fibrosis in mice. Gastroenterology. 2009; 137:1467–1477 e5. [PubMed: 19549522]
27. Ibrahim SH, Kohli R, Gores GJ. Mechanisms of lipotoxicity in NAFLD and clinical implications. J Pediatr Gastroenterol Nutr. 2011; 53:131–40. [PubMed: 21629127]
28. Ibrahim SH, Gores GJ, Hirsova P, et al. Mixed lineage kinase 3 deficient mice are protected against the high fat high carbohydrate diet-induced steatohepatitis. Liver Int. 2013
29. Aoyama T, Paik YH, Watanabe S, et al. Nicotinamide adenine dinucleotide phosphate oxidase in experimental liver fibrosis: GKT137831 as a novel potential therapeutic agent. Hepatology. 2012; 56:2316–27. [PubMed: 22806357]
30. Schwabe RF, Uchinami H, Qian T, et al. Differential requirement for c-Jun NH2-terminal kinase in TNFalpha- and Fas-mediated apoptosis in hepatocytes. FASEB J. 2004; 18:720–2. [PubMed: 14766793]
31. Peidis P, Papadakis AI, Muaddi H, et al. Doxorubicin bypasses the cytoprotective effects of eIF2alpha phosphorylation and promotes PKR-mediated cell death. Cell Death Differ. 2011; 18:145–54. [PubMed: 20559319]
32. Williams BR. Signal integration via PKR. Sci STKE. 2001; 2001:re2. [PubMed: 11752661]
33. Bai G, Hock TD, Logsdon N, et al. A far-upstream AP-1/Smad binding box regulates human NOX4 promoter activation by transforming growth factor-beta. Gene. 2014; 540:62–7. [PubMed: 24560583]
34. Jammi NV, Beal PA. Phosphorylation of the RNA-dependent protein kinase regulates its RNA-binding activity. Nucleic Acids Res. 2001; 29:3020–9. [PubMed: 11452027]
35. Ben Mosbah I, Alfany-Fernandez I, Martel C, et al. Endoplasmic reticulum stress inhibition protects steatotic and non-steatotic livers in partial hepatectomy under ischemia-reperfusion. Cell Death Dis. 2010; 1:e52. [PubMed: 21364657]
36. Cao SS, Kaufman RJ. Targeting endoplasmic reticulum stress in metabolic disease. Expert Opin Ther Targets. 2013; 17:437–48. [PubMed: 23324104]
37. Sumida Y, Niki E, Naito Y, et al. Involvement of free radicals and oxidative stress in NAFLD/NASH. Free Radic Res. 2013; 47:869–80. [PubMed: 24004441]
38. Mantena SK, King AL, Andringa KK, et al. Mitochondrial dysfunction and oxidative stress in the pathogenesis of alcohol- and obesity-induced fatty liver diseases. Free Radic Biol Med. 2008; 44:1259–72. [PubMed: 18242193]
39. Jiang JX, Venugopal S, Serizawa N, et al. Reduced nicotinamide adenine dinucleotide phosphate oxidase 2 plays a key role in stellate cell activation and liver fibrogenesis in vivo. Gastroenterology. 2010; 139:1375–84. [PubMed: 20685364]

40. Jiang JX, Chen X, Fukada H, et al. Advanced glycation endproducts induce fibrogenic activity in nonalcoholic steatohepatitis by modulating TNF-alpha-converting enzyme activity in mice. Hepatology. 2013
41. Jiang JX, Mikami K, Venugopal S, et al. Apoptotic body engulfment by hepatic stellate cells promotes their survival by the JAK/STAT and Akt/NF-kappaB-dependent pathways. J Hepatol. 2009; 51:139–48. [PubMed: 19457567]
42. Carmona-Cuenca I, Roncero C, Sancho P, et al. Upregulation of the NADPH oxidase NOX4 by TGF-beta in hepatocytes is required for its pro-apoptotic activity. J Hepatol. 2008; 49:965–76. [PubMed: 18845355]
43. Jou J, Choi SS, Diehl AM. Mechanisms of disease progression in nonalcoholic fatty liver disease. Semin Liver Dis. 2008; 28:370–9. [PubMed: 18956293]
44. Syn WK, Choi SS, Diehl AM. Apoptosis and cytokines in non-alcoholic steatohepatitis. Clin Liver Dis. 2009; 13:565–80. [PubMed: 19818305]
45. Guicciardi ME, Gores GJ. Apoptosis as a mechanism for liver disease progression. Semin Liver Dis. 2010; 30:402–10. [PubMed: 20960379]
46. Marchal JA, Lopez GJ, Peran M, et al. The impact of PKR activation: from neurodegeneration to cancer. FASEB J. 2014
47. Wang H, Xu X, Fassett J, et al. Double-Stranded RNA-Dependent Protein Kinase Deficiency Protects the Heart From Systolic Overload-Induced Congestive Heart Failure. Circulation. 2014; 129:1397–406. [PubMed: 24463368]
48. Tronel C, Page G, Bodard S, et al. The specific PKR inhibitor C16 prevents apoptosis and IL-1beta production in an acute excitotoxic rat model with a neuroinflammatory component. Neurochem Int. 2014; 64:73–83. [PubMed: 24211709]
49. Lu B, Nakamura T, Inouye K, et al. Novel role of PKR in inflammasome activation and HMGB1 release. Nature. 2012; 488:670–4. [PubMed: 22801494]
50. Haj FG, Zabolotny JM, Kim YB, et al. Liver-specific protein-tyrosine phosphatase 1B (PTP1B) re-expression alters glucose homeostasis of PTP1B−/−mice. J Biol Chem. 2005; 280:15038–46. [PubMed: 15699041]
51. Mahadev K, Motoshima H, Wu X, et al. The NAD(P)H oxidase homolog Nox4 modulates insulin-stimulated generation of H2O2 and plays an integral role in insulin signal transduction. Mol Cell Biol. 2004; 24:1844–54. [PubMed: 14966267]
52. Tiganis T. PTP1B and TCPTP--nonredundant phosphatases in insulin signaling and glucose homeostasis. FEBS J. 2013; 280:445–58. [PubMed: 22404968]
53. Subichin M, Clanton J, Makuszewski M, et al. Liver disease in the morbidly obese: a review of 1000 consecutive patients undergoing weight loss surgery. Surg Obes Relat Dis. 2015; 11:137–41. [PubMed: 25701959]
54. Sukumar P, Viswambharan H, Imrie H, et al. Nox2 NADPH oxidase has a critical role in insulin resistance-related endothelial cell dysfunction. Diabetes. 2013; 62:2130–4. [PubMed: 23349484]
55. Langhi C, Baldan A. CIDEC/FSP27 is regulated by peroxisome proliferator-activated receptor alpha and plays a critical role in fasting- and diet-induced hepatosteatosis. Hepatology. 2014

Abbreviations

HSC	hepatic stellate cells
NADPH oxidase	nicotinamide adenine dinucleotide phosphate reduced oxidase
ROS	reactive oxidative species
PKR	double-stranded RNA-activated protein kinase
ASMA	α-smooth muscle actin

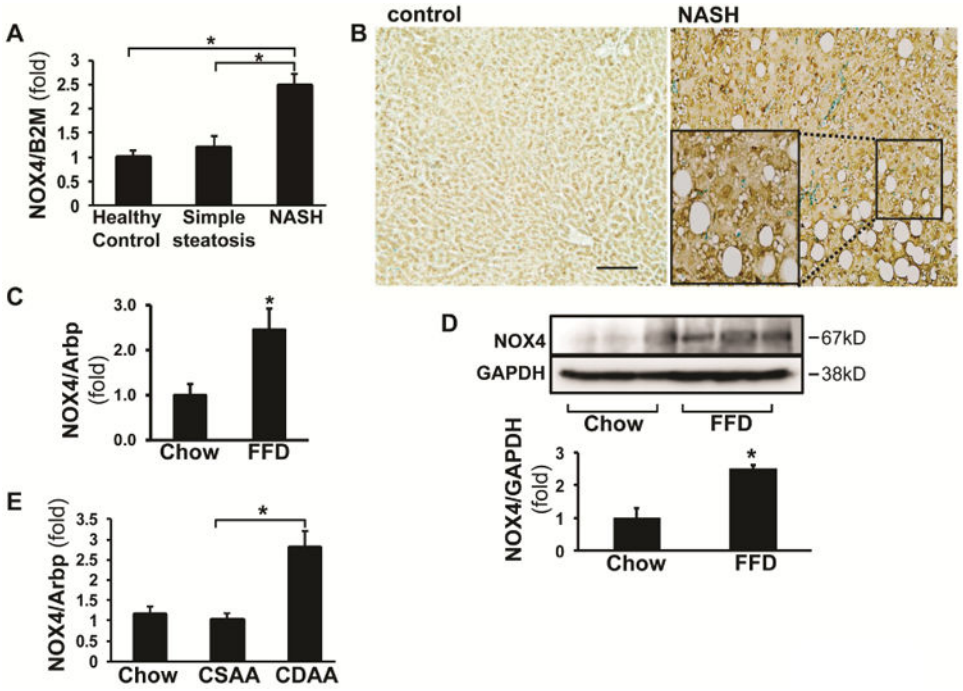

Figure 1.

NOX4 is upregulated in patients and in two dietary animal models of NASH. (**A**) RT qPCR and (**B**) immunohistochemistry were performed on the liver biopsy samples from patients with NASH, simple steatosis and healthy controls. (Data represent fold over values from healthy controls, which was set as 1, mean±SEM, N=5. For NASH patients with fibrosis stage 2-3 were included, *p<0.05). (**C**) RT qPCR was done on mouse liver samples from fast food diet (FFD), and (**D**) Representative western blot shows NOX4 induction in FFD fed mice. Densitometry, fold over chow controls, (*p<0.05). (**E**) NOX4 induction in the CDAA dietary model (fold over control values from chow-diet fed mice, N=5, *p<0.05). Scale bar: 200μm, insert scale: 50 μm.

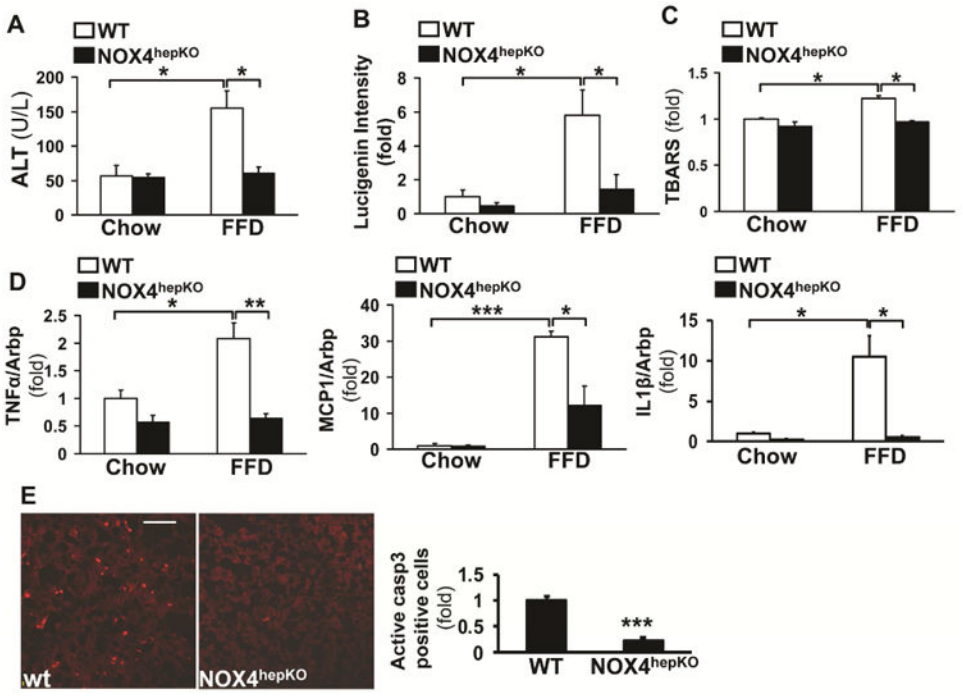

Figure 2.

Deletion of NOX4 from hepatocytes attenuated oxidative stress, lipid peroxidation, inflammation and apoptosis in mice on the fast food diet (FFD). (**A**) The serum ALT was significantly reduced in the NOX4^{hepKO} mice on the FFD (N=5 for each genotype and diet). (**B**) Oxidative radicals as assessed by the lucigenin assay decreased significantly (presented as fold over control, N=5), and (**C**) lipid peroxidation was also attenuated in the NOX4^{hepKO} mice (MDA assay, fold over control, N=5). (**D**) The expression of TNF-α, MCP1, and Il-1β showed significant decrease in the NOX4^{hepKO} mice (fold over control, N=5). (**E**) Apoptosis assessed by immunostaining for the active caspase 3 subunit on liver tissues was significantly lower in the NOX4^{hepKO} mice (counted in 5 different fields in each sample, fold over control, N=5). Values are expressed as mean±SEM, *p<0.05, **p<0.01, ***p<0.001. WT denotes littermate *fl/fl* controls, bar=200 μm.

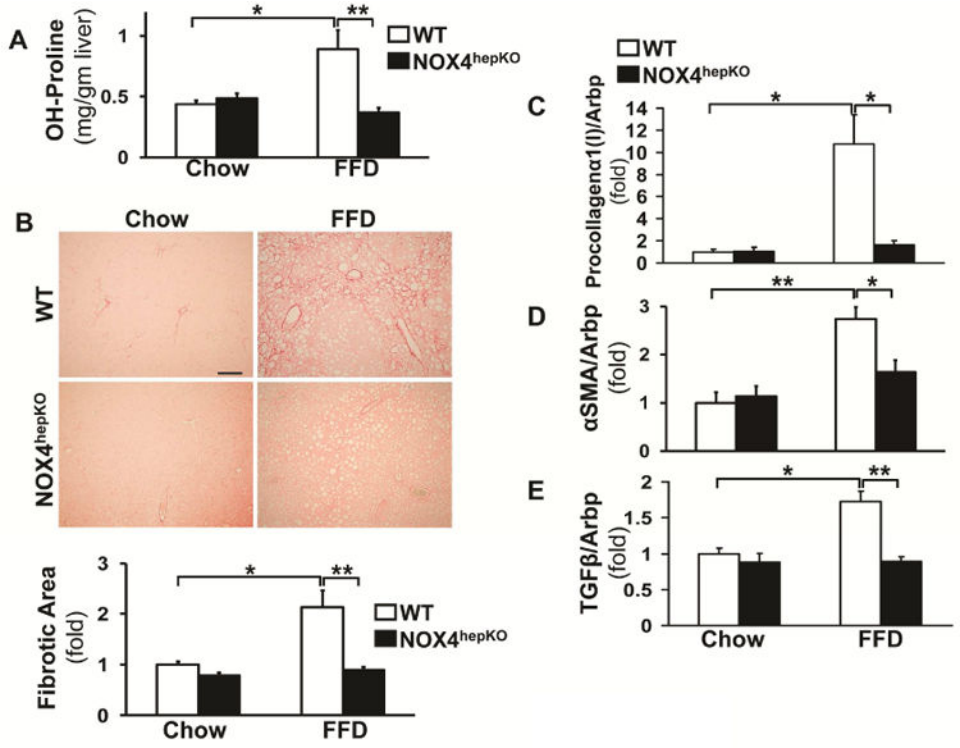

Figure 3.

Liver fibrosis decreased in the NOX4^{hepKO} mice on the fast food diet (FFD). (**A**) The amount of hydroxyproline has significantly decreased in the NOX4^{hepKO} mice on the FFD (N=5, each group), and (**B**) fibrosis visualized by picrosirius red staining and quantified by Image J analysis was reduced, as well (representative images, N=5). The expression of (**C**) procollagen α1(I), (**D**) αSMA and (**E**) TGF-β as assessed by RT qPCR was significantly decreased in the NOX4^{hepKO} mice (N=5, for each group). Values are expressed as mean ±SEM, *p<0.05, **p<0.01. WT denotes littermate *fl/fl* controls, bar=200μm.

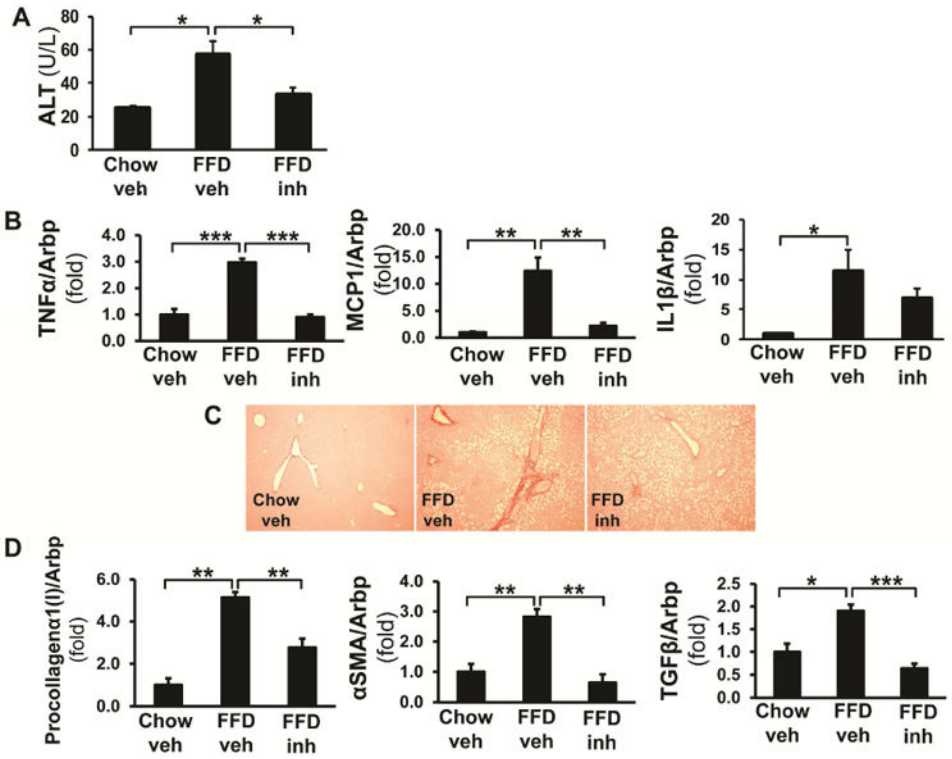

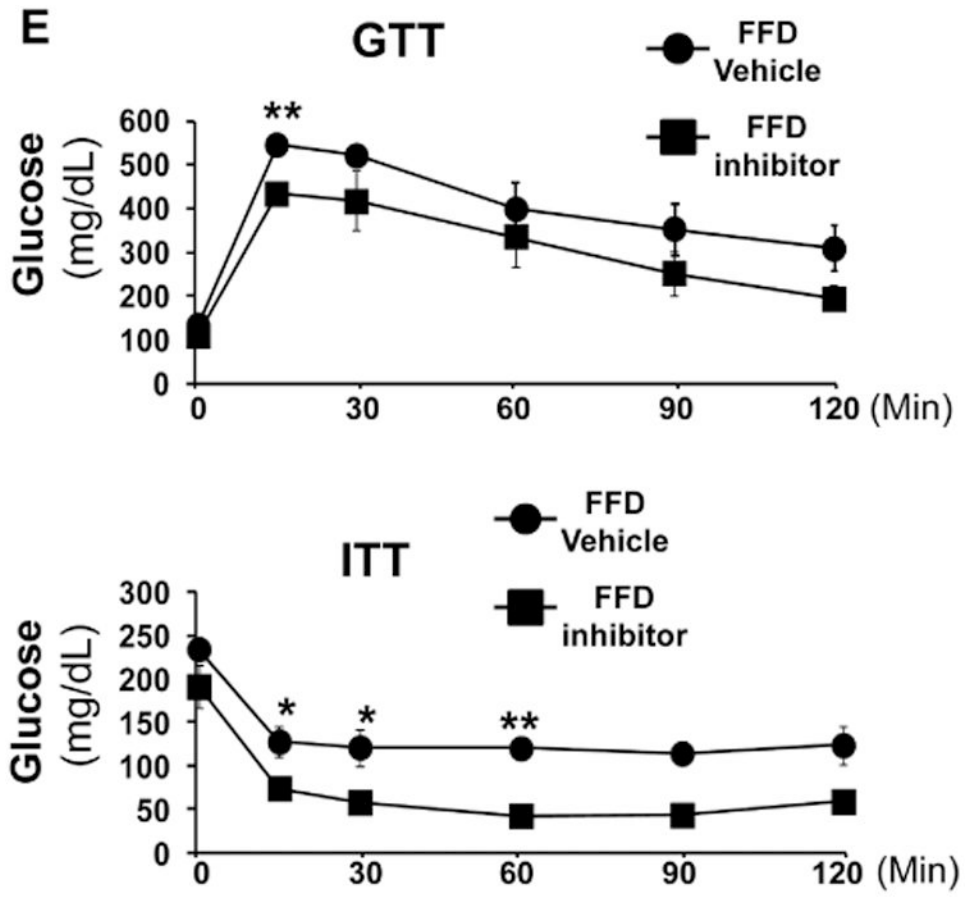

Figure 4.

Liver fibrosis and inflammation were attenuated in the GKT137831-treated fast food diet (FFD) fed mice. A group of mice were gavage-treated with either GKT137831 or vehicle from week 6 of the 12 week diet. (N=5/group). (**A**) ALT, (**B**) expression of TNF-α, MCP1, and Il-1β showed decrease in the mice treated with the inhibitor. (**C**) picrosirius red staining, and (**D**) assessment of procollagen αl(I), α SMA and TGF-β show significant improvement in fibrosis. (**E**) Total body glucose and insulin tolerance tests showed improved insulin sensitivity in the inhibitor-treated mice (veh: vehicle, inh: inhibitor *p<0.05, **p<0.01, ***p<0.001).

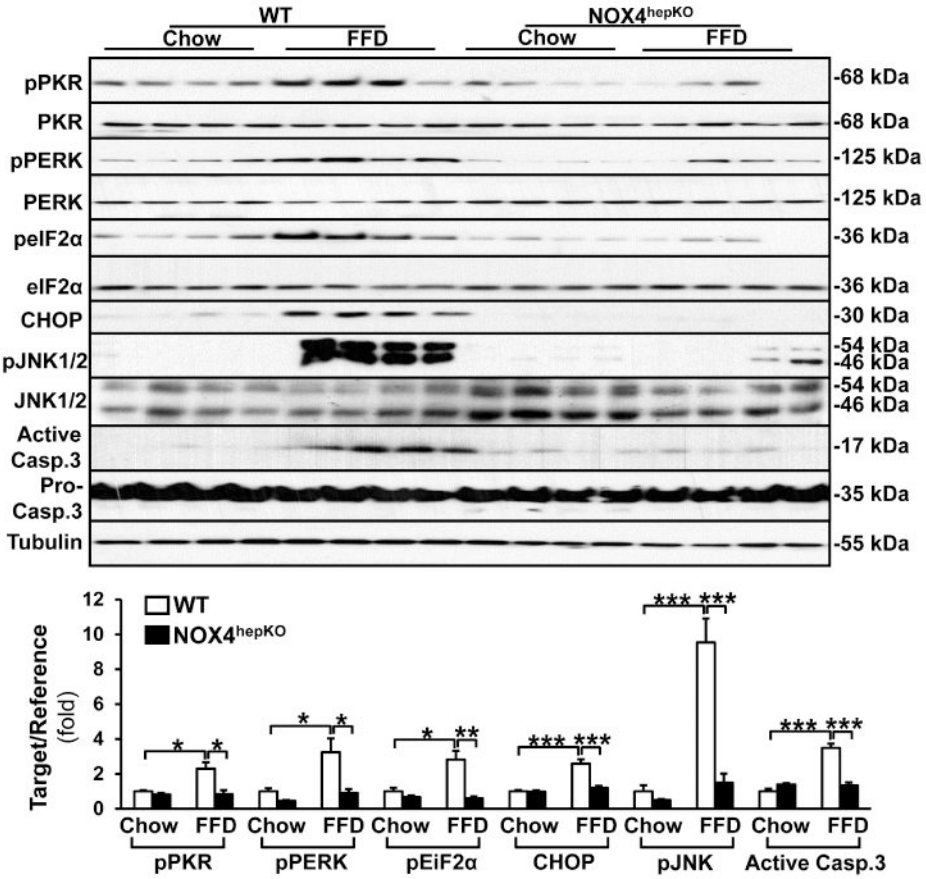

Figure 5.

NOX4^{hepKO} mice are protected against the induction of stress signaling and apoptosis during fast food diet (FFD). Representative western blot images depicting phosphorylation and activation of the double-stranded RNA-activated protein kinase (PKR), PERK, their downstream target eIF2α, CHOP, JNK1/2 and caspase 3 activation in the *fl/fl*, and NOX4^{hepKO} mice. Densitometry analysis, data are expressed as fold over control (non-phosphorylated or pro-caspase 3 values), N=5, *p<0.05, **p<0.01, ***p<0.001).

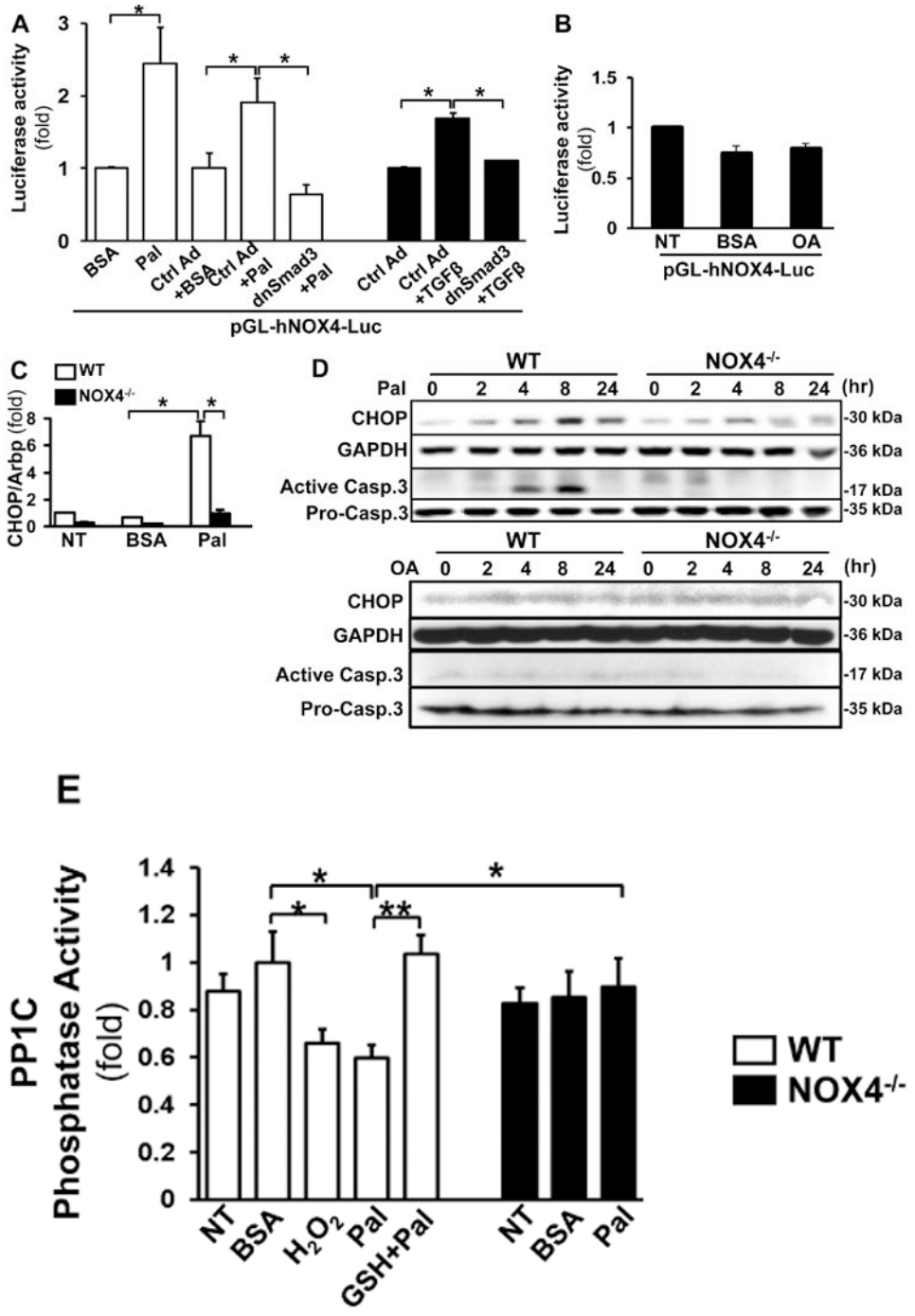

Figure 6.

Palmitate-mediated NOX4 induction in primary hepatocytes results in the attenuation of the PP1c phosphatase activity. (**A**) Luciferase promoter assays were performed by transfecting primary hepatocytes with pGL-hNOX4-Luc; transducing with Ad-GFP or Ad-DNSmad3 and exposing them to palmitate-BSA (200 μM). In parallel, promoter assays were performed in TGFβ1 (known transcriptional regulator of NOX4), ±DNSmad3-transduced hepatocytes. Palmitate treatment resulted in significant induction of the promoter activity that was

reduced by DNSmad3. (N=4, $p<0.05$). (**B**) Oleic acid (OA, 200 μM) did not induce NOX4 promoter activity (N=4). Wt (*fl/fl*) and NOX4−/− hepatocytes were exposed to palmitate-BSA. The palmitate-mediated CHOP activation both at (**C**) mRNA and (**D**) protein levels were reduced in NOX4−/− cells, and caspase 3 activation blunted (N=4 for RT qPCR and western blot). Oleic acid did not induce CHOP and caspase 3 activation. (**E**) The phosphatase activity of PP1c was studied after immunoprecipitation from palmitate-exposed primary *fl/fl* hepatocytes in the presence or absence of glutathione (GSH) or H2O2; or in the hepatocytes of NOX4−/− mice. The activity of PP1c was significantly reduced in *fl/fl* cells treated with palmitate that was restored by GSH. Treatment with H2O2 also induced a significant decrease in phosphatase activity. There was no reduction in the PP1c activity after palmitate treatment in the $NOX4^{-/-}$ hepatocytes (NT: no treatment, N=4). (Ctr Ad: Ad-GFP, Values are expressed as fold over control, mean±SEM, *$p<0.05$, **$p<0.01$).

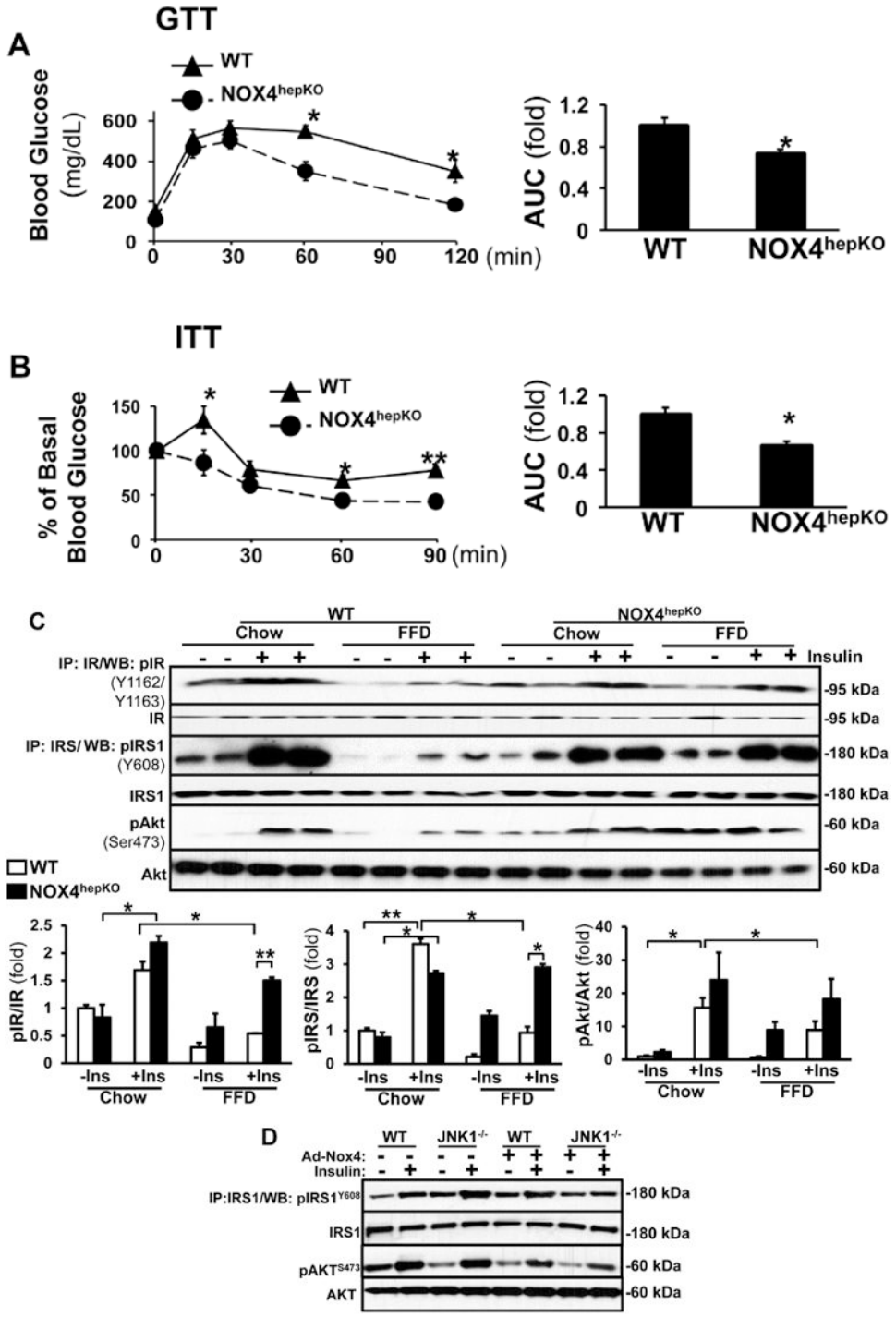

Figure 7.

Insulin sensitivity and signaling are improved in the NOX4^{hepKO} mice on the fast food diet. (FFD) (**A**) glucose (GTT) and (**B**) insulin tolerance tests (ITT) were performed and the NOX4^{hepKO} mice had improved overall insulin sensitivity compared to wt (*fl/fl*) controls (N=5 for each group, AUC: area under the curve, values are expressed as fold over control, mean±SEM, *p<0.05, **p<0.01). (**C**) *fl/fl* or NOX4^{hepKO} mice on the FFD were given

insulin, and immunoprecipitation/western blot performed to assess IR, IRS-1, and western blots to test Akt phosphorylation. The phosphorylation of IR, IRS-1, and Akt improved in the NOX4^{hepKO} mice compared to *fl/fl* mice (representative blots, N=4, Densitometry, values are expressed as fold over control, mean±SEM, *p<0.05, **p<0.01). **(D)** NOX4 induction in JNK1KO hepatocytes reduces IRS1^{Tyr608} and Akt^{Ser473} phosphorylation in response to insulin compared to control vector-transduced cells. Wt or JNK1KO primary hepatocytes were transduced with Ad-GFP or Ad-NOX4 for 24 hours then exposed to 100nM insulin and IRS-1 immunoprecipitated and blotted for IRS$^{\mathbf{tyr608}}$**.** Akt western blotting performed to detect pAKT^{S473}. The Hyperinsulinemic-euglycemic clamp studies are depicted in Suppl. Fig. 8.

Table 1

Primer sequences used in the real time qPCR studies.

Antibody	Vendor	Catalog Number
α-smooth muscle actin	Abcam	Ab7817
Akt	Cell Signaling	9272
Phospho-Akt (Ser 473)	Cell Signaling	4060
Cleaved Caspase-3 (Asp175)	Cell Signaling	9664
Caspase-3	Cell Signaling	9662
CHOP 10(GADD 153)	Santa Cruz Biotechnology	Sc-575
Cytokeratin 19	Abcam	Ab7755
E-cadherin	BD Biosciences	610182
elF2α	Abcam	Ab26197
Phospho-elF2α (pS^{52})	Invitrogen	44728G
GAPDH	Life Technologies	AM4300
Insulin receptor (IR)	Santa Cruz Biotechnology	SC711
Phospho-IR (pYpY$^{1162/1163}$)	Invitrogen	44-804G
IRS1,pre CT	Millipore	06-526
Phospho-IRS1 (pTyr 608)	Millipore	PS1010
JNK	Cell Signaling	9252
Phospho-JNK (Thr183/Tyr185)	Cell Signaling	9251
NOX4	A gift from Dr. Ajay Shah	
PERK	Santa Cruz Biotechnology	Sc-13073
Phospho-PERK(Thr981)	Santa Cruz Biotechnology	Sc-32577
PKR	Santa Cruz Biotechnology	Sc-1702
Phospho-PKR(Thr451)	Millipore	07-886
PTP1B	Millipore	07-088
TCPTP	Abcam	Ab180764
β-Tubulin	Santa Cruz Biotechnology	Sc-5274

Table 2

Antibodies used in the studies

Fat, %	20.0
Total Saturated fatty Acids, %	12.09
Total Monosaturated Fatty Acids, %	4.61
Polyunsaturated Fatty Acids, %	0.58
Protein, %	17.4
Carbohydrates, %	49.9
Fiber, %	5

Table 3
Components of the AIN-76A Western Diet (supplemented with fructose: FFD)

Human N0X4	Forward: 5′-GATGTTGGGGCTAGGATTGTGTC-3′
	Reverse: 5′-AAAAGGATAAGGCTGCAGTTGAG-3′
Human B2M	Forward: 5′-TTCTGGCCTGGAGGCTATC-3′
	Reverse: 5′-TCAGGAAATTTGACTTTCCATTC-3′
Mouse NOX4	Forward: 5′-TTGCCTGGAAGAACCCAAGT-3′
	Reverse: 5′-TCCGCACAATAAAGGCACAA-3′
Mouse	Forward: 5′-AGAGGCGAAGGCAACAGTCG-3′
Procollagen α1(I)	Reverse: 5′-GCAGGGCCAATGTCTAGTCC-3′
Mouse αSMA	Forward: 5′-TCAGCGCCTCCAGTTCCT-3′
	Reverse: 5′-AAAAAAAACCACGAGTAACAAATCAA-3′
Mouse TGFβ	Forward: 5′-CATGGAGCTGGTGAAACGG-3′
	Reverse: 5′-GCCTTAGTTTGGACAGGATCTGG-3′
Mouse TNFα	Forward: 5′-TCCCAGGTTCTCTTCAAGGGA-3′
	Reverse: 5′-GGTGAGGAGCACGTAGTCGG-3′
Mouse MCP1	Forward: 5′-CTTCTGGGCCTGCTGTTCA-3′
	Reverse: 5′-CCAGCCTACTCATTGGGATCA-3′
Mouse IL-1β	Forward: 5′-CAACCAACAAGTGATATTCTCCATG-3′
	Reverse: 5′-GATCCACACTCTCCAGCTGCA-3′
Mouse SREBP1c	Forward: 5′-GGAGCCATGGATTGCACATT-3′
	Reverse: 5′-GCTTCCAGAGAGGAGGCCAG-3′
Mouse FAS	Forward: 5′-ATGTGAACAGCGCAGGCAC-3′
	Reverse: 5′-ACAATGCCCACGTCACCAAT-3
Mouse PPARγ	Forward: 5′-TCTTAACTGCCGGATCCACAA-3′
	Reverse: 5′-GCCCAAACCTGATGGCATT-3′
Mouse CD36	Forward: 5′-TCCAGCCAATGCCTTTGC-3′
	Reverse: 5′-TGGAGATTACTTTTTCAGTGCAGAA-3′
Mouse CHOP	Forward: 5′-CCAGCAGAGGTCACACGCAC -3′
	Reverse: 5′-CTGGGCACTGACCACTCTGTTTC-3′
Mouse Arbp	Forward: 5′-CAAAGCTGAAGCAAAGGAAGAG-3′
	Reverse: 5′-AATTAAGCAGGCTGACTTGGTTG-3′